

Mössbauer study of a magnetic ordering in the FeNiCrMoSiB metallic glass

M. MIGLIERINI*

Department of Nuclear Physics and Technology, Slovak Technical University, Mlynská Dolina, CS-812 19 Bratislava, Czechoslovakia

The influence of varying amount of chromium on magnetic ordering of amorphous $\text{Fe}_{30}\text{Ni}_{48-x}\text{Cr}_x\text{Mo}_2\text{Si}_5\text{B}_{15}$ is studied by transmission Mössbauer spectroscopy. Mössbauer data are fitted considering the asymmetry of the lines using the NORMOS DIST programs. Distributions of hyperfine parameters are constructed by a histogram method. Bimodal character of $P(H)$ distributions is observed also at liquid nitrogen temperature. Concentration dependent creation of the central doublet points out the low-field peak in $P(H)$ to dominate. Clustering of Cr atoms at the Fe sites is supposed to be the main reason for this effect. Simple model of a 3-D $P(H)$ projection is introduced.

1. Introduction

In recent years, Mössbauer measurements of various chromium containing metallic glasses (MGs) were reported [1–10]. Mössbauer spectroscopy is a common technique in the study of Fe-based amorphous materials. The information obtained from the Mössbauer spectra only refers to the local structure around the iron atoms. Particularly, hyperfine field distribution (HFD), known as a $P(H)$ distribution, and quadrupole splitting distribution, $P(QS)$, are of special interest. The former because of its unusual bimodal character which is a point of controversy in the literature [2, 6] while the latter appears frequently (with respect to an amount of Cr) in room temperature studies [7, 9].

A two-peak HFD structure arises from the presence of a central doublet in addition to a ferromagnetic sextet at $T < T_C$ [1]. The central doublet is often fitted by means of unresolved sextuplets although the iron atoms with hyperfine fields of less than 5T should be treated as non-magnetic [4]. This is a weak point of such fitting procedures yielding some doubts about the existence of the second maximum in $P(H)$ [1, 6, 11]. Moreover, bimodal HFDs have been found to be out of the validity region proposed by LeCaër *et al.* [12]. In spite of this it is generally accepted that small hyperfine fields do exist [2, 6] even though their origin is not clear [1, 3].

In a previous paper [9] the problem of a shape for room temperature Mössbauer spectra and $P(H)$ distributions while the composition of amorphous $\text{Fe}_{30}\text{Ni}_{48-x}\text{Cr}_x\text{Mo}_2\text{Si}_5\text{B}_{15}$ varies, was considered. It was shown there how an increase of the chromium content x reduces ferromagnetic exchange interactions giving rise to a total magnetic long-range order collapse into a pure paramagnetic behaviour beyond $x = 8$. In addition, a fall of chemical short-range order (SRO) observed implies a compositional dependent

decrease of Curie temperature [8, 10].

The aim of the present paper is to study an influence of chromium on a local SRO using an analysis of $P(H)$ distributions. Varying amounts of Cr would be helpful in obtaining further insight into the problem and enable the creation of the central doublet to be observed. For that reason Mössbauer spectra have been taken sufficiently down below T_C . Any information on SRO needs a fitting procedure based on a theoretical model of the local neighbourhood of the iron atoms. The spectra were evaluated by the NORMOS DIST programs developed by Brand [13] considering the asymmetry of the lines. Room temperature measurements are also reported. As it will be shown, the results indicate that an increase of x leads to a clustering of chromium in the vicinity of Fe atoms which in turn reduces an average value of an HFD. Concentration dependent shape features of $P(H)$ distributions are demonstrated by means of simple 3-D graphs.

2. Experimental procedure

Ribbon-shaped samples (thickness 16–27 μm , width 6 mm) of amorphous $\text{Fe}_{30}\text{Ni}_{48-x}\text{Cr}_x\text{Mo}_2\text{Si}_5\text{B}_{15}$ for $x = 0, 2, 4, 6, 8, 10$ and 12 were prepared by the melt-spinning method at the Institute of Physics, Slovak Academy of Sciences in Bratislava. Their amorphousness was checked by X-ray diffraction and Mössbauer spectroscopy.

Conventional constant acceleration Mössbauer spectrometer with ^{57}Co (Rh) source was used in transmission geometry. The spectra were recorded at room (295 K) and liquid nitrogen (78 K) temperature. Calibration of the apparatus was performed using a 12.5 μm natural iron foil produced by AMERSHAM Ltd.

To fit the Mössbauer spectra the NORMOS DIST program was applied [13]. $P(H)$ and $P(QS)$ distributions were constructed by the histogram method (DISTRI = 1) from up to 35 sextets and 15 doublets,

* Present address: Department of Material Physics, Osaka University, Toyonaka, Osaka 560, Japan

respectively, a line width of 0.27 mm s^{-1} was assumed. Spectrum asymmetries were covered by introducing a linear change in isomer shift (METHOD = 2, resp. 6) and by the parameters related to a SRO (I_p , H_{1p} , Q_p , H_{2p}) for magnetically split patterns.

3. Results and discussion

3.1. Room temperature measurements

Fig. 1 illustrates room temperature Mössbauer spectra of the amorphous $\text{Fe}_{30}\text{Ni}_{48-x}\text{Cr}_x\text{Mo}_2\text{Si}_5\text{B}_{15}$ along with the corresponding hyperfine distributions. Noticeable changes of magnetic ordering with respect to Cr content, x , are clearly seen on the shapes of Mössbauer spectra. Primary six-line patterns which characterize ferromagnetic ordering are being continuously transformed owing to x -dependent changes in exchange interactions into a pure doublet. This behaviour can also be observed on the shapes of corresponding hyperfine distributions. It should be noted here, that the hyperfine distributions for $x = 10$ and 12 are in fact $P(QS)$ distributions [7]. They are, however, recalculated and redrawn in the same H -scale as the other $P(H)$ ones for the purpose of a mutual qualitative comparison. Y-axes are reduced by a factor of 4. Average values and standard deviations of the distributions are listed in Table 1 and they are plotted against chromium content, x , in Figs 2 and 3, respectively.

Looking at the $P(H)$ distributions one can observe some traces of their bimodality even for $x = 0$ when no chromium is present in the sample. It may be due

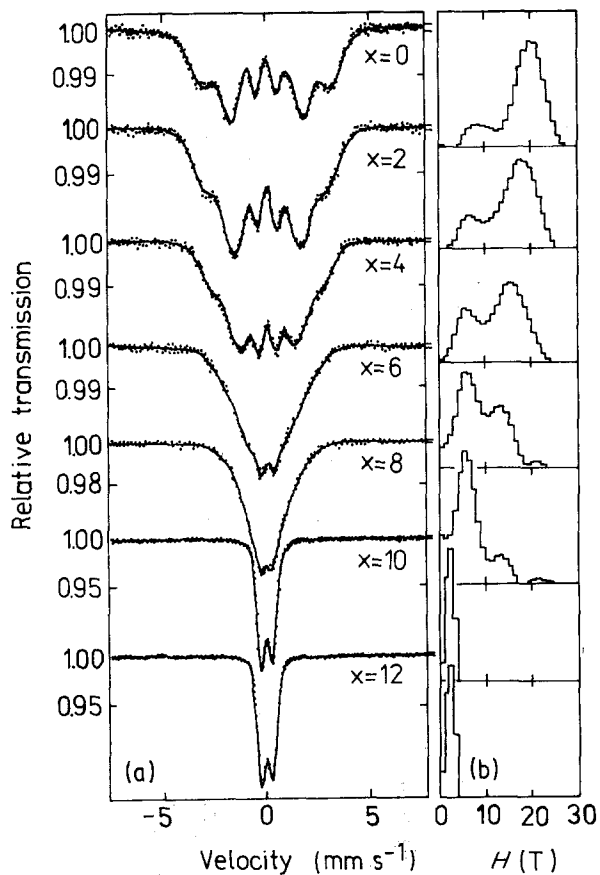


Figure 1 $\text{Fe}_{30}\text{Ni}_{48-x}\text{Cr}_x\text{Mo}_2\text{Si}_5\text{B}_{15}$ metallic glass: (a) Mössbauer spectra taken at room temperature with changing chromium content, x , and (b) corresponding hyperfine distributions.

TABLE 1 Parameters of the hyperfine field distributions as derived from room and liquid nitrogen temperature Mössbauer spectra of the $\text{Fe}_{30}\text{Ni}_{48-x}\text{Cr}_x\text{Mo}_2\text{Si}_5\text{B}_{15}$ metallic glass: $\langle H \rangle$, average value and ΔH , standard deviation given in tesla. The figure enclosed in brackets shows the error in the last digit.

Sample x	Room temperature		Liquid nitrogen temperature	
	$\langle H \rangle$	ΔH	$\langle H \rangle$	ΔH
0	17.08(5)	4.99(7)	22.0(1)	6.1(1)
2	14.84(4)	5.10(7)	20.8(1)	6.5(1)
4	12.09(5)	5.17(9)	19.1(1)	6.5(1)
6	8.33(8)	4.4(2)	17.6(1)	6.9(1)
8	6.35(7)	4.3(2)	16.4(1)	7.4(1)
10	0.531(6) ^a	0.25(1) ^a	14.8(1)	7.3(1)
12	0.525(7) ^a	0.26(1) ^a	13.6(2)	7.4(2)

^a Values of quadrupole splitting distribution: $\langle QS \rangle$, average value and ΔQS , standard deviation given in mm s^{-1}

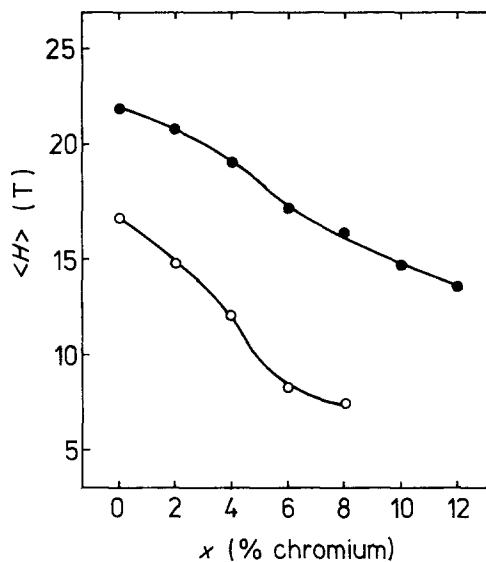


Figure 2 A mean magnetic hyperfine field value, $\langle H \rangle$, plotted against chromium content, x , of the $\text{Fe}_{30}\text{Ni}_{48-x}\text{Cr}_x\text{Mo}_2\text{Si}_5\text{B}_{15}$ metallic glass. Data were obtained from room (O) and liquid nitrogen (●) temperature Mössbauer spectra.

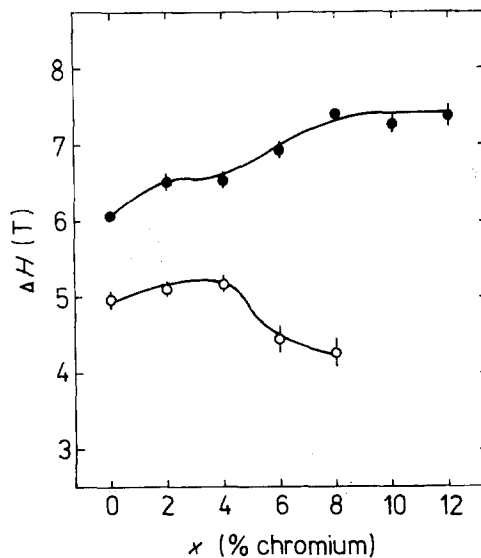


Figure 3 Standard deviation of a hyperfine field distribution, ΔH , plotted against chromium content, x , of the $\text{Fe}_{30}\text{Ni}_{48-x}\text{Cr}_x\text{Mo}_2\text{Si}_5\text{B}_{15}$ metallic glass. Data were obtained from room (O) and liquid nitrogen (●) temperature Mössbauer spectra.

to molybdenum which is in the same column of the periodic table as Cr [5, 14].

The shifts of both peaks towards low H values in connection with a vanishing of the high-field component (Fig. 1) and a consequent rapid decrease of $\langle H \rangle$ (open dots in Fig. 2) indicate changes in a chemical SRO [7, 15]. They may be caused by a clustering of non-magnetic Cr atoms in the iron sites. Decrease of Ni amount with rising x should be taken into account as well. Consequently, Fe–Cr pairs tend to prevail over the Fe–Fe and Fe–Ni ones [5]. This is also evident from the Mössbauer spectra where the central doublet becomes more dominant and the ferromagnetic sextet disappears. To have a closer look on the low-field tail of a $P(H)$ distribution and/or the central part, Mössbauer spectra below the magnetic ordering temperature have been taken.

3.2. Liquid nitrogen temperature measurements

Purely resolved and fully overlapped room temperature Mössbauer spectra for $x = 6$ and 8 are hard to fit. Moreover, because of a paramagnetic behaviour of the samples for $x = 10$ and 12 no HFD could have been obtained at all in this case. To overcome this disadvantage the temperature of the experiment was lowered sufficiently below T_C to 78 K. The actual values of T_C can be found elsewhere [10]. Mössbauer spectra achieved are seen in Fig. 4 along with the $P(H)$ distributions.

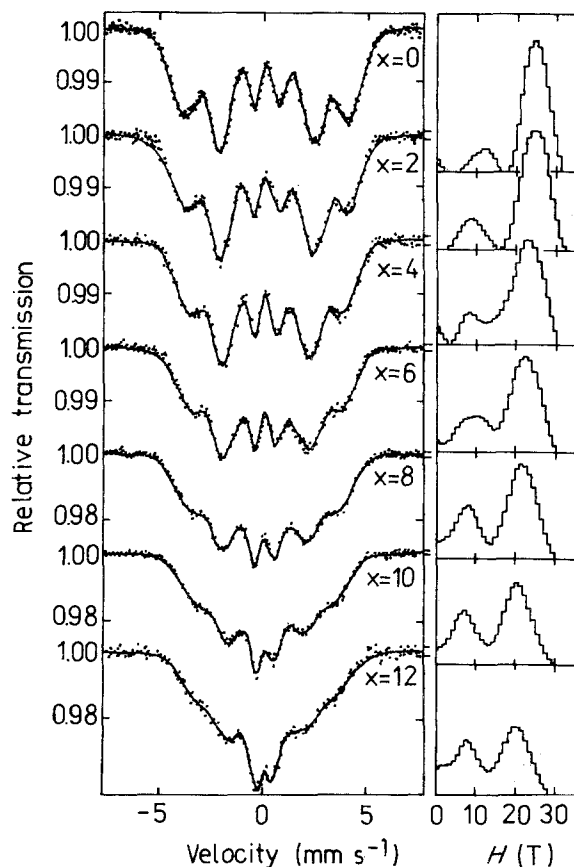


Figure 4 $\text{Fe}_{30}\text{Ni}_{48-x}\text{Cr}_x\text{Mo}_2\text{Si}_3\text{B}_{15}$ metallic glass: (a) Mössbauer spectra taken at 78 K with changing chromium content, x , and (b) corresponding hyperfine field distributions.

The spectra exhibit six-line patterns with more or less, depending on x , pronounced central parts and the $P(H)$ distributions are bimodal in shape. The origin of the high-field component of a HFD is clear enough since it is related to a magnetically split phase in the sample whereas the low-field one could be assigned to the central doublet in a Mössbauer spectrum. The latter increases in intensity as Cr concentration is increased.

Characteristic parameters of $P(H)$ distributions are collected in Table 1 and shown in Figs 2 and 3. Higher average values of HFDs than those achieved at room temperature were expected and they are a consequence of a $T^{3/2}$ -law [16]. Concentration dependence of a mean value, $\langle H \rangle$, (full dots in Fig. 2) depicts a similar feature as that at room temperature (open dots) and may be explained likewise. Continuous increase of a standard deviation, ΔH , (full dots in Fig. 3) points out a decrease of SRO for liquid nitrogen temperature measurements. On the other hand, from the falling ΔH -values (open dots in Fig. 3), a rising importance of quadrupole interactions in the vicinity of a magnetic ordering temperature can be considered.

A creation of the central doublet is seen in the Mössbauer spectra. This indicates changes in a magnetic ordering due to concentration induced rearrangements of the atoms in the nearest neighbourhoods of iron. Consequently, a chemical SRO is affected [7, 15] causing the ferromagnetic exchange interactions to weaken. In addition, decrease of an in-plane anisotropy while the Cr content increases may be expected [8]. Because of the fitting problems associated with a strong line overlap, it can be quantified using the standard spectra only which can be achieved e.g. by the magic angle method [8, 17]. To support the previous assumption plots of the relative areas, D23, of the second and the fifth Mössbauer lines against Cr content for both room and liquid nitrogen temperature measurements (Fig. 5) can be presented.

Domain structure and hence orientations of magnetic moments are governed by a magnetic anisotropy. Having in mind that the magnetic moment orientations are directly reflected through D23 the

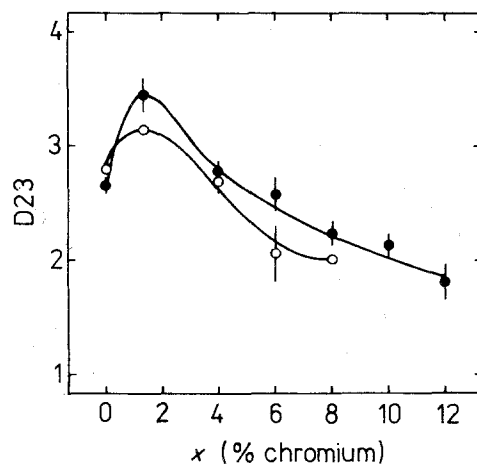


Figure 5 Relative area, D23, of the second and the fifth lines of: (a) room (\circ) and (b) liquid nitrogen (\bullet) temperature Mössbauer spectra of the $\text{Fe}_{30}\text{Ni}_{48-x}\text{Cr}_x\text{Mo}_2\text{Si}_3\text{B}_{15}$ metallic glass plotted against Cr content, x .

concentration dependences in Fig. 5 suggest changes in magnetic anisotropy. The increase of D23 between $x = 0$ and 2 is probably caused by an addition of chromium to the base alloy. The following fall of D23 implies a tendency of magnetic moments to turn out of the ribbon plane.

3.3. 3-D graphs of hyperfine distributions

To reveal concentration dependent deviations in a local SRO induced by a varying amount of Cr the $P(H)$ distributions should be analysed. For that reason simple 3-D projections of hyperfine fields as shown in Figs 6 and 7 are introduced. Normalized $P(H)$ distributions are stacked into files according to an increasing chromium content yielding the second concentration dimension to be established. The use of the histogram method is quite convenient in this case.

The influence of Cr on the shapes of HFDs can be observed in a more illustrative way by means of such plots. A rapid increase of the low-field component is seen in the room temperature 3-D graph (Fig. 6) implying changes in SRO as they have been discussed above. Again, the sharp peak in the high concentration corner is in fact ascribed to the redrawn $P(QS)$ distributions. Thus, one can clearly observe the ferro-to paramagnetic transition beyond $x = 8$. Complete vanishing of the high-field hump also supports this consideration. Moreover, both humps are shifted towards low H values with the rising amount of chromium. From the qualitative point of view the same behaviour of HFDs is demonstrated in Fig. 7 when the amorphous $\text{Fe}_{30}\text{Ni}_{48-x}\text{Cr}_x\text{Mo}_2\text{Si}_5\text{B}_{15}$

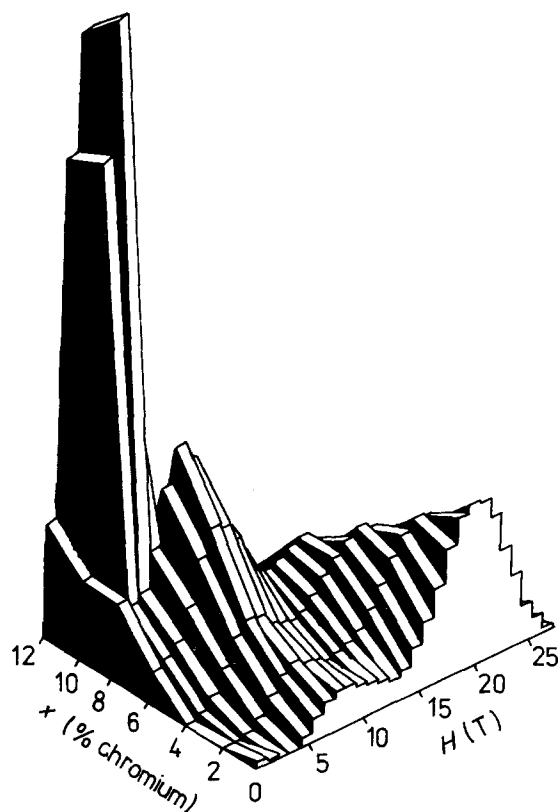


Figure 6 3-D $P(H)$ distributions corresponding to the room temperature Mössbauer spectra of the amorphous $\text{Fe}_{30}\text{Ni}_{48-x}\text{Cr}_x\text{Mo}_2\text{Si}_5\text{B}_{15}$.

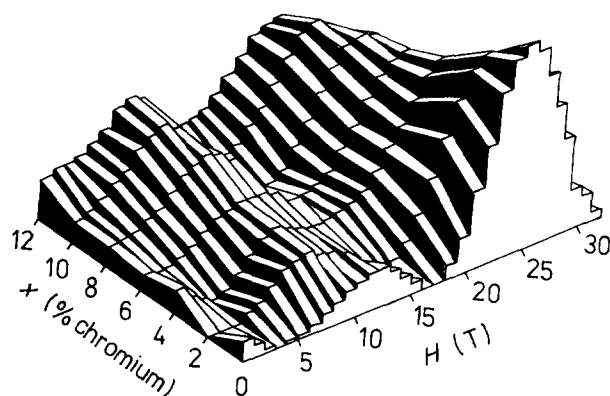


Figure 7 3-D $P(H)$ distributions corresponding to the liquid nitrogen temperature Mössbauer spectra of the amorphous $\text{Fe}_{30}\text{Ni}_{48-x}\text{Cr}_x\text{Mo}_2\text{Si}_5\text{B}_{15}$.

occurs below the magnetic ordering temperature. The two-hump character is clearly resolved and its existence at this low temperature favours quadrupole interactions to prevail.

4. Conclusions

The analysis of HFDs in a wide concentration range elucidated some of the factors which govern the magnetic ordering of the amorphous $\text{Fe}_{30}\text{Ni}_{48-x}\text{Cr}_x\text{Mo}_2\text{Si}_5\text{B}_{15}$. The Mössbauer spectra have been taken both at room and liquid nitrogen temperature. Bimodal $P(H)$ distributions have been obtained using the NORMOS DIST fitting programs.

An increase of chromium in the samples causes the possibility of these atoms to occupy more and more of the iron nearest-neighbouring sites to dominate. Assuming also a decreasing amount of Ni, a continuous vanishing of the ferromagnetic exchange interactions can be observed with a total magnetic long-range order collapse into a pure paramagnetic behaviour beyond $x = 8$ at room temperature. The increase of the low-field component is supposed to be a consequence of a clustering of chromium atoms. Due to molybdenum a two-peak $P(H)$ structure is seen even in the sample without chromium.

From the creation of well pronounced central doublets in the Mössbauer spectra taken at liquid nitrogen temperature, a rising importance of quadrupole interactions for higher amounts of chromium is concluded. 3-D $P(H)$ projections have been introduced. They were found to be helpful for a shape analysis of the concentration dependence of the hyperfine distributions studied.

Acknowledgement

Dr R. A. Brand (Jülich, FRG) is gratefully acknowledged for providing his NORMOS programs and V. Švehlík for the help with implementing them.

References

1. M. PIECUCH, G. MARSCHAL, Ph. MANGIN and Chr. JANOT, *Phys. Status. Solidi (a)* **62** (1980) K99.

2. G. L. WHITTLE, S. J. CAMPBELL and A. M. STEWART, *Phys. Status. Sol. (a)* **71** (1982) 245.
3. G. RAJARAM, S. PRASAD, G. CHANDRA, S. N. SHRINGI and R. KRISHNAN, *Phys. Lett.* **98A** (1983) 57.
4. Yu. BOLIANG, J. M. D. COEY, M. OLIVIER and J. O. STRÖM-OLSEN, *J. Appl. Phys.* **55** (1984) 1748.
5. A. M. STEWART and G. L. WHITTLE, in "Rapidly Quenched Metals" edited by S. Steeb and H. Warlimont, (North-Holland 1985) p. 553.
6. R. V. VADNERE, V. SRINIVAS, A. K. NIGAM, G. RAJARAM, G. CHANDRA, S. PRASAD, S. N. SHRINGI and R. KRISHNAN, *Hyperfine Interact.* **42** (1988) 955.
7. R. A. DUNLAP, D. W. LAWTHOR, P. HARGRAVES and P. SINCLAIR, *J. Phys. F: Met. Phys.* **18** (1988) 2479.
8. P. AURIC, J. M. GRENECHE, O. deBOUVIER and J. J. RAMEAU, *J. Magn. Magn. Mater.* **82** (1989) 243.
9. M. MIGLIERINI, *J. Mater. Sci. Lett.* **9** (1990) 497.
10. M. MIGLIERINI, J. SITEK, L. MACKO, M. MIHALIK and A. ZENTKO, *Hyperfine Interact.* **60** (1990) 695.
11. R. A. BRAND, *Nucl. Instr. Meth. Phys. Res.* **B28** (1987) 398.
12. G. LeCAËR, J. M. DUBOIS, H. FISCHER, U. GONSER and H. G. WAGNER, *Nucl. Instr. Meth.* **B5** (1984) 25.
13. R. A. BRAND, NORMOS programs, Internal Report, Angewandte Physik, Universität Duisburg.
14. C. L. CHIEN and H. S. CHEN, *J. Appl. Phys.* **50** (1979) 1574.
15. P. HARGRAVES and R. A. DUNLAP, *J. Magn. Magn. Mater.* **75** (1988) 378.
16. S. PRASAD, G. CHANDRA, G. RAJARAM, V. SRINIVAS, S. N. SHRINGI and R. KRISHNAN, *J. Magn. Magn. Mater.* **54-57** (1986) 259.
17. J. M. GRENECHE and F. VARRET, *J. Phys. C: Solid State Phys.* **15** (1982) 5333.
18. J. M. GRENECHE and F. VARRET, *Solid State Commun.* **54** (1985) 985.

*Received 9 July
and accepted 6 November 1990*